2022

Modeling and Performance Evaluation of Rotary Compressor and Air-Conditioning System using Low GWP Refrigerants

Hana Sano

Eriko Urasaki

Tao Lyu

Jongsoo Jeong

Kenji Tojo

See next page for additional authors

Modeling and Performance Evaluation of Rotary Compressor and Air-Conditioning System using Low GWP Refrigerants

Hana SANO*, Eriko URASAKI, Tao LYU, Jongsoo JEONG, Kenji TOJO, Yonezou IKUMI, Hiroo NAKAMURA, Seiichi YAMAGUCHI, Kiyoshi SAITO

WASEDA University, Department of Mechanics and Aerospace Engineering
3-4-1Okubo, Shinjuku-ku, Tokyo, Japan
(Phone:+813-5286-2941, Email:flower-87@toki.waseda.jp)

* Corresponding Author

ABSTRACT

As social awareness toward global warming grows, conventional refrigerants are regulated in stages. In order to select safe and environmentally friendly next-generation refrigerants for highly efficient heat pump system, a performance evaluation method by simulation technologies must be properly established due to limitation of experiment by extensive refrigerants. In this study, we first focused on refrigerant behavior inside a rotary compressor that strongly influences system performance, and developed detailed simulation models that accounts for the effects of leakage and heat transfer of refrigerant with lubricant. In addition, compressor performance tests were conducted to verify the validity of the model. Finally, heat pump cycle simulations were carried out using the compressor efficiencies, and the effects of different refrigerant properties such as R410A and Low GWP refrigerants on the characteristics and performance of the entire heat pump cycle was clarified.

1. INTRODUCTION

As worldwide interest toward global warming has grown, countries and organizations have issued regulations and commitments to gradually regulate the usage of conventional refrigerants with high global warming potential (GWP) in refrigeration and air-conditioning systems, such as the Paris Agreement (United Nations, 2015) and the Kigali Amendment (United Nations, 2016). With the current refrigerants being regulated in stages, we must choose alternative refrigerants. Next-generation refrigerants must be assessed and selected as to not only conform the safety standards and environmental impact, but also deliver high-performance when applied to the systems. To select the appropriate next-generation refrigerant and propose possible refrigerants that could appropriately meet the criteria from a large number of options, it is foremost demanded to comprehensively evaluate its usage on the target applications. In this study, we will focus on the compressor, which is one of the elements of a heat pump that has a significant impact on the cycle performance as consumes the highest power.

We evaluated the performance of a rotary compressor theoretically and experimentally for low GWP refrigerants, and the results were used to simulate the overall performance of an air conditioning system. The refrigerants used in this study are R410A as the baseline and being widely used, R32 which is currently the mainstream, and R466A which is attracting attention as a next-generation refrigerant. A model of the compressor is constructed considering the effects of leakage and heat transfer of the refrigerant and lubricant. Compressor simulations based on the model are performed to calculate the state changes inside the compression chamber, and to clarify the effects of differences in refrigerant properties on compressor characteristics and performance. In addition, the compressor was experimentally tested for R410A and R32 with the parameters of superheat degree, rotation speed, suction pressure, and discharge pressure in the actual rotary compressor. The validity of the developed model is verified by comparing the performance test results with the simulation results. Finally, heat pump cycle simulations were performed based on the compressor simulation model to clarify the effects of different refrigerants on the overall heat pump cycle performance, and to discuss the effects of refrigerant properties on compressor performance and cycle performance.

2. MODELING

2.1 Compression Chamber Model

A positive displacement compressor for refrigerant draws refrigerant gas into the compression chamber, reduces its volume by mechanical power, and discharges it to a higher pressure. The simulation technology has been widely used with the development of rotary compressors (Shimizu *et al.*, 1975), (Tojo *et al.*, 1978), (Yanagisawa *et al.*, 1982), (Fukuta *et al.*, 1995). A simulation model was constructed with reference to them. In the process of compressing the gas, due to heat, mass, and work transfer, the state of the refrigerant in the compression chamber continuously changes in time. As shown in Fig. 1, the amount of work given to the compressed refrigerant, leakages between adjacent chambers with different pressures, heat transfers between gas, wall surface, and lubricant are considered. In addition, gas and lubricant do not change in phase, and the specific volume of lubricant does not change with pressure. It is further assumed that the lubricant behaves like an immiscible mist contained in the gas and there is no heat transfer between the lubricant and the wall surface.

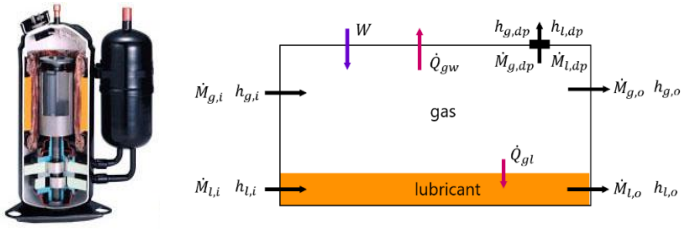

Figure 1: Compression chamber model

2.2 Fundamental Equations

The energy and mass conservation of the gas and lubricant in the compression chamber can be expressed in Equation (1)-(4).

$$\frac{dM_g u_g}{dt} = \dot{M}_{g,i} h_{g,i} - \left(\dot{M}_{g,o} + \dot{M}_{g,dp}\right) h_{g,o} + \dot{W} - \dot{Q}_{gw} - \dot{Q}_{gl} \tag{1}$$

$$\frac{dM_l u_l}{dt} = \dot{M}_{l,i} h_{l,i} - \left(\dot{M}_{l,o} + \dot{M}_{l,dp}\right) h_{l,o} + \dot{Q}_{gl} \tag{2}$$

$$\frac{dM_g}{dt} = \dot{M}_{g,i} - \dot{M}_{g,o} - \dot{M}_{g,dp} \tag{3}$$

$$\frac{dM_l}{dt} = \dot{M}_{l,i} - \dot{M}_{l,o} - \dot{M}_{l,dp} \tag{4}$$

2.3 Leakage

The area of the clearance is obtained from geometric relationships based on Shimizu *et al*. (1975) and Yanagisawa *et al*. (1982) listed in the reference. The amount of leakage is calculated by using the apparent specific heat ratio and gas temperature, assuming thermal equilibrium and the homogeneity of the two-phase flow of gas and lubricant, as in the model of Fujiwara *et al*. (1985). For the mixture of refrigerant and lubricant, the lubricant is always included in the mass fraction φ. The mass flow rate of leaked gas and lubricant flowing through the gap of the high-pressure side, Chamber 1, to the low-pressure side, Chamber 2, (the leakage path ① and ② shown in Fig.2) is calculated by Equation (7), which is the mass flow rate of a compressible fluid passing through an orifice. Apparent specific heat ratio of the mixture is obtained by Equation (9). The mass flow rate of leaked lubricant flowing through the leakage path ③ and ④ shown in Fig.2 is calculated by Equation (10).

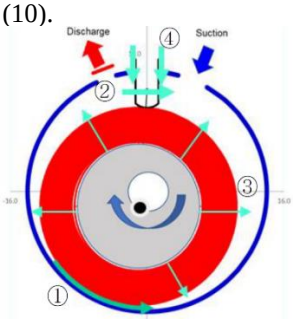

Figure 2: Leakage path of rotary compressor

$$\dot{M}_g = (1-\varphi)\dot{M} \tag{5}$$

$$\dot{M}_l = \varphi\dot{M} \tag{6}$$

$$\dot{M} = \begin{cases} cA\sqrt{\dfrac{2\kappa}{\kappa-1}P_1\rho_1\left\{\left(\dfrac{P_2}{P_1}\right)^{\frac{2}{\kappa}} - \left(\dfrac{P_2}{P_1}\right)^{\frac{\kappa+1}{\kappa}}\right\}} & (P_2 > P_{\mathrm{ch}}) \\ cA\sqrt{\kappa P_1\rho_1\left(\dfrac{2}{\kappa+1}\right)^{\frac{\kappa+1}{\kappa-1}}} & (P_2 \le P_{\mathrm{ch}}) \end{cases} \tag{7}$$

$$P_{\mathrm{ch}} = P_1\left(\frac{2}{\kappa+1}\right)^{\frac{\kappa}{\kappa-1}} \tag{8}$$

$$\kappa = \frac{C_p M_g + C_l M_l}{C_v M_g + C_l M_l} \tag{9}$$

$$\dot{M}_l = \frac{b\rho_l}{12lv_l}(P_{in} - P_{out})\delta^3 \tag{10}$$

2.4 Heat Transfer

Heat transfer area between the gas and the wall is equivalent to the inner surface area of the compression chamber, which is the sum of top, bottom, and side surfaces can be determined by the geometric parameters. Heat transfer coefficients between the refrigerant and the wall surface are calculated by the Nusselt number using the equation for the forced convection heat transfer in a circular tube. (Kays and Crawford, 1980)

$$\dot{Q}_{gl} = h_{gl}S_{gl}(T_g - T_l) \tag{11}$$

$$\dot{Q}_{gw} = h_{gw}S_{gw}(T_g - T_w) \tag{12}$$

$$Nu = CRe^m Pr^n (C = 0.022, m = 0.8, n = 0.5) \tag{13}$$

3. SIMULATION METHOD

3.1 Compressor Simulation

Based on the model in the previous section, simulations are performed using R410A, R32, and R466A refrigerants, assuming a rotary compressor for a residential R410A air-conditioning system, to clarify the effect of refrigerant properties on compressor characteristics and performance. Table 2 shows the properties of each selected refrigerant, including the theoretical COP, specific heat ratio before compressor suction, density, cooling effect, and other major physical properties of the theoretical cycle under the conditions shown in Table 1. The refrigerant state quantities from suction to discharge are calculated for each angle on MATLAB using the Runge-Kutta method along with the boundary conditions at the inlet and outlet of the compressor. Under the conditions shown in Table 3, volumetric efficiency, adiabatic efficiency, suction completed temperature, and discharge temperature are calculated by changing the condensing temperature. The change in the amount of leakages between adjacent chambers and heat transfer from compression chamber wall to refrigerant gas are visualized at the condensing temperature is of 42℃. Refrigerants properties are obtained from REFPROP10.

Table 1: Operating Condition

Super heat	℃	5
Sub cool	℃	3
Evaporating temperature	℃	8.5
Condensing temperature	℃	42

Table 2: Properties of Refrigerant

Refrigerant	R410A	R32	R466A
Composition (Mass %)	R32/R125=50/50wt%	R32=100wt%	R32/R125/CF3I =49/11.5/39.5wt%
GWP (AR4)	2090	675	733
Safety classification	A1	A2L	A1
Specific heat ratio	1.38	1.49	1.43
Density ($kg \cdot m^{-3}$)	38.5	27.8	45.8
Cooling effect($kJ \cdot kg^{-1}$)	165	250	149
Cooling effect($kJ \cdot m^{-3}$)	6374	6953	6837
Theoretical COP	6.65	6.81	6.71
COP ratio based on R410A	1.00	1.02	1.01

Table 3: Specifications of compressor simulation

Displacement volume	cc	7.25
Rotational speed	rps	60
Evaporating temperature	℃	8.5
Super heat	℃	5
Lubricant circulating ratio	%	2.0

3.2 Heat Pump Cycle Simulation

Using the volumetric and adiabatic efficiencies calculated in Section3.1, cycle simulation of a residential R410A air-conditioning unit for R410A, R32, and R466A refrigerants is carried out to clarify the effect of refrigerant properties on heat pump cycle performance. We use EF+M (Ohno and Saito, 2012), (Wada et *al.*, 2021) simulation platform which enables convenient system analysis even when the refrigerant or refrigerant circuit is changed and calculate heat pump cycle COP and cooling capacity under the condition of Table 4. As shown in Table 5, the displacement volume is determined to meet the cooling capacity of 2.8 kW and charge amount of the refrigerant is set to maximize the COP. The cooling capacity and COP of each refrigerant were calculated by varying the outdoor temperature.

Table 4: Specifications of heat pump cycle simulation

Cooling capacity		kW	2.8
Compressor	Rotational speed	rps	60
Indoor fan	Power consumption	W	20
Outdoor fan		W	40
Indoor temperature	DB	℃	27
	WB	℃	19
Outdoor temperature	DB	℃	35
	WB	℃	24

Table 5: Condition of calculation

Refrigerant	Mass charge	Displacement volume
	kg	cc
R410A	0.87	7.25
R32	0.66	6.80
R466A	0.92	7.20

4. RESULTS AND CONSIDERATION

4.1 Leakage and Heat Transfer

Figure 3 shows the leakage flow rate through each leakage path shown in Figure 2 at the condensation temperature of 42 °C. The vertical axis is the ratio of the leakage mass flow rate to the refrigerant mass in the compression chamber at the end of suction, and the horizontal axis is the rotational angle from the start of suction. The influence of heat

transfer is also shown in Fig. 4. The vertical axis is the ratio of the heat transfer to the heat capacity of the refrigerant in the compression chamber at the end of suction, and the horizontal axis is the rotational angle from the start of suction. As shown in Fig. 3 and 4, the effects of leakage and heat transfer on compressor characteristics were found to be greater with R32 than with other refrigerants.

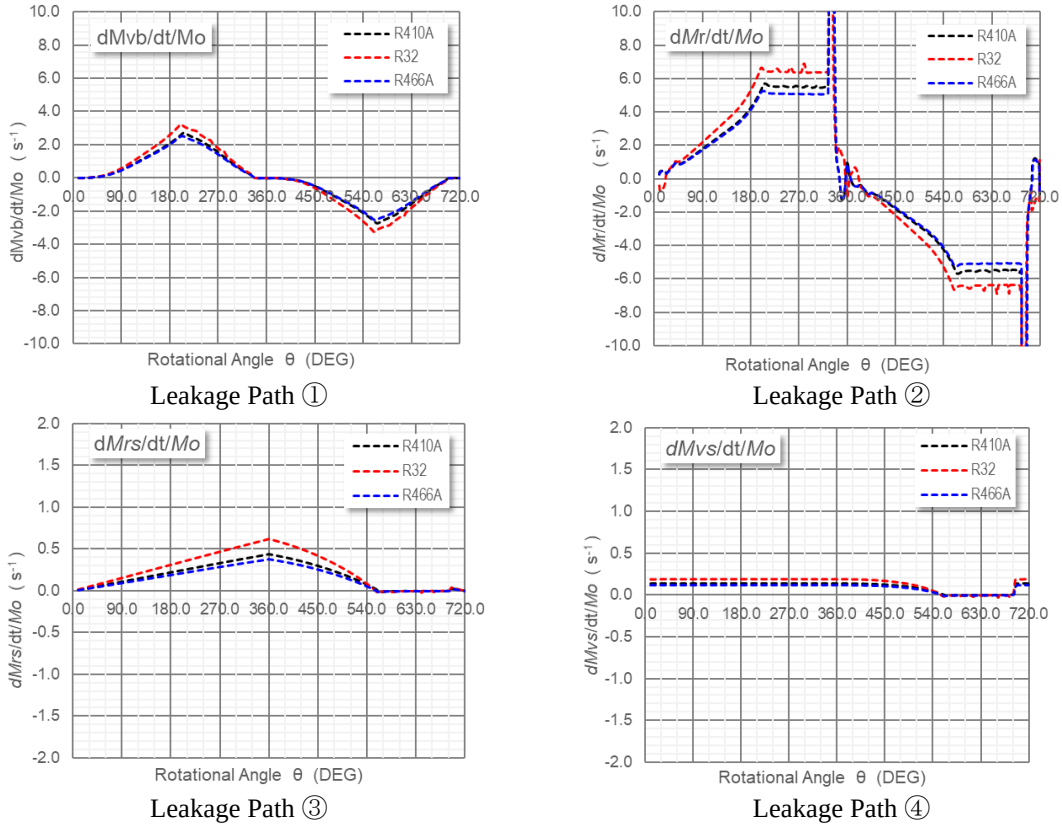

Figure 3: Leakage flow rate through 4 different leakage paths

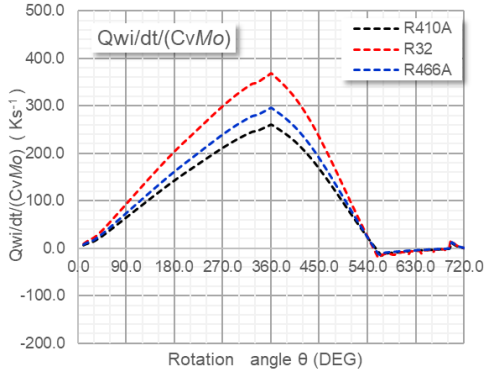

Figure 4: Heat transfer between gas and compression chamber wall

4.2 Performance of Compressor

Volumetric efficiency, adiabatic efficiency, suction completed temperature and discharge temperature at different condensing temperatures are shown in Fig. 5. The horizontal axis is compression ratio, which is the ratio of the discharge pressure to the suction pressure. Volumetric efficiency increases with decreasing compression ratio, and adiabatic efficiency reaches its maximum at a pressure ratio of 1.8~2.0. For R32, volumetric efficiency is 2~5% and adiabatic efficiency is 1~2% lower than those of R410A. When R466A was used, the volumetric efficiency was almost the same as that of R410A, and the adiabatic efficiency was about 1% higher in the large compression ratio region.

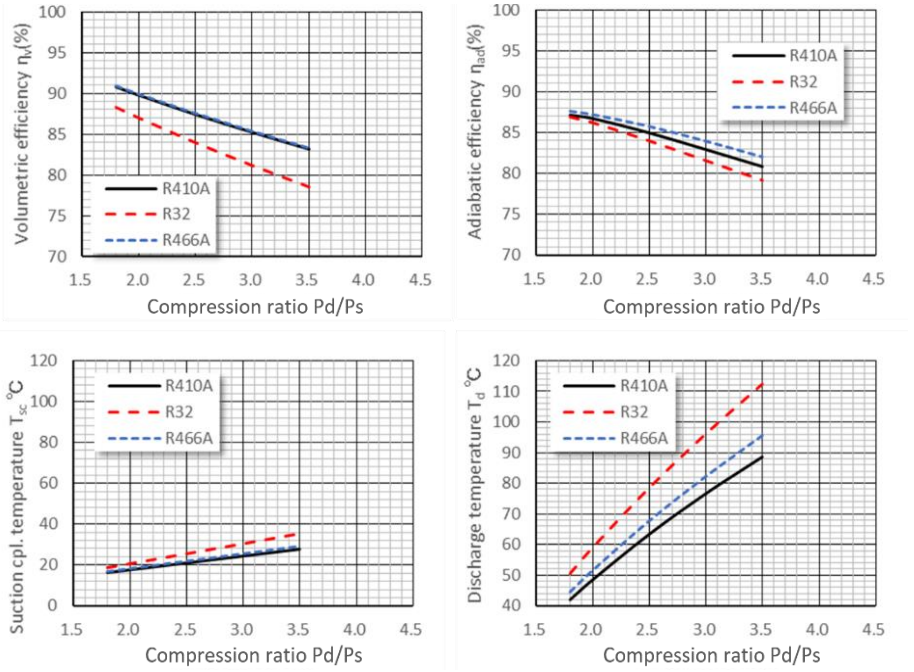

Figure 5: Performance of compressor

4.3 Comparison of Compressor Performance Test and Simulation

To validate the simulations, compressor performance test was carried out with R410A and R32 under the same conditions shown in table 3 with the pressure ratio as a parameter at 60 Hz. The volumetric efficiency and total compressor efficiency are shown in Fig. 6. In both cases, the volumetric and total compressor efficiencies tended to decrease with increasing pressure ratio. The volumetric efficiency with R32 was 2~4% lower than that with R410A, showing good agreement between the simulation and experimental results. On the other hand, the compressor total efficiency with R32 was slightly lower than that with R410A in the simulation results, while the experimental results showed almost the same characteristics. The differences in these compressor characteristics will be further investigated.

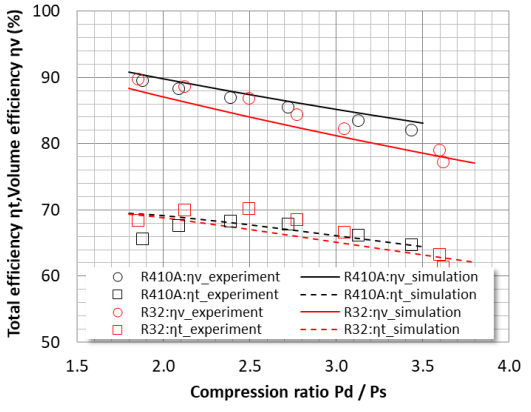

Figure 6: Result of performance test and simulation

4.4 Heat Pump Cycle Simulation

Fig. 7 show the simulation results of the cooling capacity and COP respectively, with different outdoor air temperatures. It was found that the COP and cooling capacity decreased as the outdoor temperature increased. The COP of R32 was 4~5% higher than that of R410A, and COP of R466A was 1~2% lower than that of R410A. In addition, under higher outdoor air temperature conditions, R32 provided slightly higher cooling capacity than that of R410A and R466A

Both the volumetric and total efficiencies of R32 were slightly lower than those of R410A in the compressor simulation, but higher cycle COP was obtained in the cycle simulation. This is thought to be due to the small density

of R32 and its high refrigeration effect. The higher refrigeration effect results in a smaller circulating mass flow rate of refrigerant at the same cooling capacity, which leads to smaller pressure losses in the evaporator and inlet connection piping and higher evaporation pressure, which in turn results in smaller compressor power and ultimately higher cycle COP with R32.

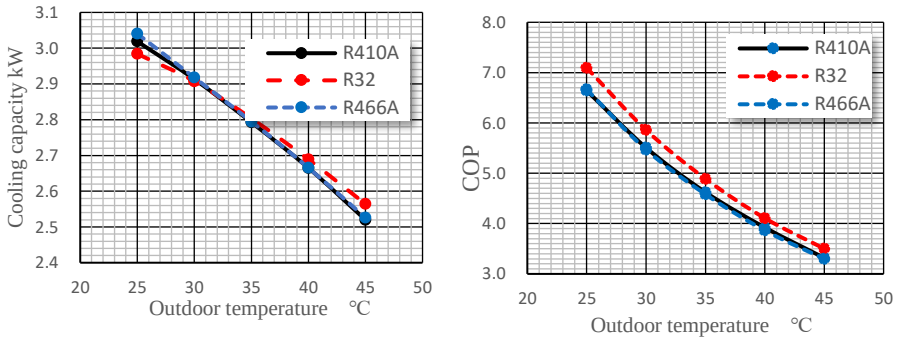

Figure 7: Results of heat pump cycle simulation

5. CONCLUSIONS

In this study, compressor simulations, performance tests, and heat pump cycle simulations were conducted for a residential room air conditioner using three types of refrigerants (R410A, R32, and R466A), and the following conclusions were obtained.

- The results of the compressor simulation showed that volumetric efficiency and adiabatic efficiency of R32 were 2~5% and 1~2% lower than those of R410A, respectively. On the other hand, volumetric efficiency of R466A was almost the same as that of R410A, and adiabatic efficiency was 0~2% higher.
- The volumetric efficiency with R32 and R4410A showed good agreement between the simulation and experimental results.
- The heat pump cycle simulation results showed that the COP of R32 was 4~5% higher than that of R410A. The COP of R466A was 1~2% lower than that of R410A.

NOMENCLATURE

A	area of clearance	(m^2)	u	specific internal energy	($kJ \cdot kg^{-1}$)
b	gap width	(m)	V	volume	(m^3)
C	specific heat	($kJ \cdot kg^{-1} \cdot K^{-1}$)	W	work	(kJ)
c	flow coefficient	(–)	Pr	Prandtl number	(–)
h	specific enthalpy	($kJ \cdot kg^{-1}$)	Nu	Nusselt number	(–)
h	heat transfer coefficient	($kW \cdot m^{-2} \cdot K^{-1}$)	Re	Reynolds number	(–)
l	gap length	(m)	η	efficiency	(–)
M	mass	(kg)	θ	rotational angle	(rad)
P	pressure	(Pa)	κ	specific heat ratio	(–)
Q	heat transfer	(kJ)	ν	kinematic viscosity	(m^2/s)
S	surface	(m^2)	ρ	density	($kg \cdot m^{-3}$)
T	temperature	(K)	φ	mass ratio	(–)
t	time	(s)	δ	gap height	(m)

Subscript

ad	adiabatic	o	out
ch	choke	p	pressure
d	discharge	s	suction
dp	discharge port	sc	suction completed
g	gas	th	theoretical
i	in	v	volume
l	lubricant	w	wall

REFERENCES

[1] Fujiwara M., Kasuya K., Matsunaga T., Watanabe M., “Performance Analysis of Screw Compressor”, Trans. Jpn. Soc. Mech. Eng., Vol.51, No.466, pp1816-1824 (1985). (in Japanese)
[2] Fukuta M., Yanagisawa T., Shimizu T., Shikata T., “Compression Characteristics of Refrigerant-Oil Mixture in Refrigerant Compressors (1st Report, Modeling of Leakage and Heat Transfer)”, Trans. Jpn. Soc. Mech. Eng., Vol.61, Vol.582, pp542-548 (1995).
[3] Ohno K., Saito K., Proceedings of the 46th Japanese Joint Conference on Air-conditioning and Refrigeration, 119(2012).
[4] Shimizu T., Shiga T., Tyuu I., “Some Investigation on the Pressure Change Characteristics of a Rotary Compressor”, Refrigerantion, Vol.50, No.573, pp7-14 (1975).
[5] Tojo K., Kan T, Arai A., “Dynamic Behavior of Sliding Vane in Small Rotary Compressors", Proc of the 3rd Int. Comp. Eng. Conf. at Purdue (1978).
[6] W. M. Kays and M. E. Crawford, Convective Heat and Mass Transfer, McGraw-Hill, (1980), pp. 238-248.
[7] Wada E., Lyu T., Tojo K., Ikumi Y., Nakamura H., Saito K., “Evaluating Compressor Performance with Low-GWP Refrigerants by Simulation Model”, Proc of the 25th Int. Comp. Eng. Conf. at Purdue (2021).
[8] Yanagisawa T., “Leakage loss of rolling piston type rotary compressor (1)”, Trans. Jpn. Soc. Mech. Eng., Vol.48, No.426, pp265-274 (1982). (in Japanese)
[9] Yanagisawa T., Shimizu T., Nakamura M., “Leakage loss of rolling piston type rotary compressor (2)”, Trans. Jpn. Soc. Mech. Eng., Vol.48, No.431, pp1256-1265 (1982). (in Japanese)

ACKNOWLEDGEMENT

This research project was done as the commissioned work (JPNP18005) of the New Energy and Industrial Technology Development Organization (NEDO). We would like to express our gratitude here.